Optimisation of industrial production of low-force sensors – adhesive bonding of force-centring ball

T Maeder, C Jacq, M Blot, and P Ryser

Laboratoire de Production Microtechnique (LPM), École Polytechnique Fédérale de Lausanne (EPFL), CH-1015 Lausanne, Switzerland

thomas.maeder@epfl.ch

Abstract. This work addresses the issue of attaching the force-centring part (a round ball) to the load cell of a force sensor, a piezoresistive thick-film Wheatstone bridge deposited onto a ceramic cantilever. As the current soldering process requires expensive metallisation steps for both the ball and the cantilever, and subjects the solder pads used for mounting the cantilever to an additional reflow cycle, an alternative adhesive bonding process was developed, allowing both simpler production and the use of other ball materials such as ceramic and glass. The self-centring action of solder capillary forces was ensured by structuring the adhesive so as to form a mechanical cuvette allowing centring of the ball by gravity. The selected adhesive materials exhibited good printability and bonding, as well as surviving the subsequent soldering and cleaning process steps.

1. Introduction

1.1. Simple cantilever-type thick-film force sensor

Mechanical load (pressure and force) sensors based on the piezoresistive properties of thick-film (TF) resistors have found wide application due to their robustness and simple, straightforward manufacture [1-5]. We have developed [5-7] a basic low-range force sensor (figure 1) with an alumina cantilever that also acts as the load cell. For lower forces, LTCC (low-temperature cofired ceramic) technology, having a lower elastic modulus, being available in thin sheets and amenable to 3D structuration, has allowed fabrication of a more responsive variant of the sensor by replacing the alumina cantilever with an LTCC one (figure 2) [8-11].

1.2. Motivation of present work

Production of these sensors is quite straightforward, with the overall process flow listed in table 1. Most processes fall within the bounds of standard TF / LTCC technology and other usual procedures in electronics, such as surface-mount technology (SMT) using solder attachment. However, the solder pads of the cantilever, which are used for mechanically bonding and electrically interconnecting it to the base, currently experience three solder reflow operations: 1) pre-tinning those pads, 2) soldering the force-centring ball, and 3) soldering the cantilever to the base. This exposes the pads to considerable leaching by and reaction with solder, an issue that has been considerably exacerbated by the introduction of lead-free soldering based on tin-rich solders [12,13].

Therefore, the object of the present work, which has been carried out in the frame of a student project [14] and complemented by additional experiments is to examine the possibility of replacing the ball soldering process (table 2) by adhesive bonding (table 3), which promises several advantages:

- Gluing eliminates one solder reflow step, decreasing the thermal / metallurgical budget of the bottom cantilever solder pads to 2 vs. 3 reflow operations.
- No special metallisation of the ball or cantilever is necessary (the thick-film conductive tracks on the cantilever do not allow soldering by themselves).
- A wider range of ball materials may in principle be used, including low-cost glass balls, which also have the advantage of having a low thermal conductivity (lower influence of the temperature of the contact surface on the signal) and being electrically insulating (lower influence of noise sources coupled through the contact surface)

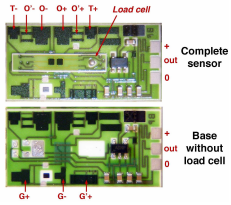

Figure 1. Basic low-force sensor with alumina cantilever (the letters denote positions of laser trimming cuts); from [7].

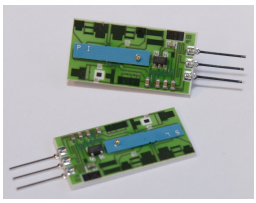

Figure 2. Force sensor, variant with LTCC cantilever (in blue); from [10].

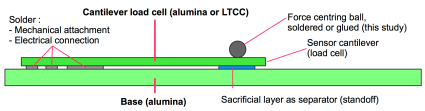

Figure 3. Assembly principle of cantilever onto base, with solder pads (left side) as a permanent electrical and mechanical connection [7] and a sacrificial layer (right, tip side) as a temporary separator.

Table 1. Overall force sensor fabrication process flow.

#	Main process phase	Description
1	Deposition of circuit on base	Standard TF deposition onto alumina substrate
2	Deposition of piezoresistive load-cell bridge on cantilever	TF deposition onto 0.25-0.635 mm thick alumina substrate, or LTCC process with co-fired TF layers
3	Coarse trimming of load cell	Laser offset trimming & stabilisation by annealing
4	Pre-tinning of load cell pads	Solder screen printing & reflow
5	Assembly of force-centring ball onto load cell	Soldering (current) or adhesive bonding – ***object of present work***
6	Individualisation of cantilevers	Breakage of pre-scored cantilever substrate
7	Mounting of components onto base, including cantilever	SMT process, with lead-free SAC (Sn-Ag-Cu) solder & sacrificial-layer cantilever separator (figure 3)
8	Active sensor trimming	Laser trimming with force applied by custom jig
9	Cleaning	Ultrasound bath – solder flux cleaning & sacrificial-layer removal
10	Individualisation of sensors	Breakage of pre-scored sensor base substrate
11	Final steps	Optional lead attachment and inspection

Table 2. Ball attachment onto cantilever - process steps for soldering.

#	Process step	Description
1	Additional thick-film metallisation layer on top side of cantilever	Standard TF process[a b]
2	Metallisation of steel ball	Etching, followed by electroless nickel / immersion gold (ENIG) metallisation[c]
3	Deposition of "wet" solder	Screen / stencil printing
4	Mounting of ball	Mechanical "sieve"[d]
5	Solder reflow[e]	Reflow oven

[a] A conductor layer on the cantilever top side is either not present (LTCC) or too thin to allow soldering (alumina), requiring deposition of a specific solderable metallisation.
[b] The metallisation of the attachment pads on the bottom side of the cantilever must also be better (i.e. more expensive) than in case of adhesive bonding, because it has to survive three vs. two reflow steps, but this only requires a thicker layer, not an additional one.
[c] Necessary to allow solderability of the chromium steel bearing ball (EN 1.3505 / 100Cr6).
[d] Balls are simply "sieved" over a plate with holes corresponding to their correct position on each cantilever. A standard component pick-and-place machine has also been used.
[e] Second solder reflow operation to the cantilever solder pads, after tinning (see table 1).

Table 3. Ball attachment onto cantilever - process steps for adhesive bonding.

#	Process step	Description
1	Deposition + cure of 'cuvette' formulation	Screen printing + thermal cure
2	Deposition of wet 'glue' formulation	Screen printing, same screen as (1)
3	Mounting of ball	Mechanical "sieve" (see table 2, note d)
4	Curing of adhesive	Box oven[bc]

2. Requirements and selected approach

2.1. Requirements

To be validated as a replacement for soldering, the adhesive bonding process must meet the following requirements:

1) Correct positioning of the balls (ensured by capillary forces for the soldering process)
2) Sufficient lateral shear strength, at least ~4 N (a conservative requirement, as the maximum vertical nominal force range measured by the sensor is 2 N)
3) Simple, straightforward process steps, as few as possible, with low cost of materials
4) Compatibility with subsequent steps: acceptable strength conserved after cantilever mounting (solder reflow at ~260°C) and cleaning (exposure to solvents)
5) Acceptable compression strength of ball (if the current steel ball is replaced)

2.2. Adhesive deposition process and basic materials category

We chose screen printing as the adhesive application method, for several reasons: good integration within the TF production process (mostly screen printing), parallel deposition (large amount of cantilevers, 180 per substrate), and deposition capability for thick films in one print (thickness needed to achieve a good contact area with the round ball, see also figure 4). This choice, however, restricts

the acceptable range of adhesives to those materials that have a sufficiently long screen / pot life: adhesives curing with ambient moisture or two-part ones with fast ambient temperature cure should be avoided. Additionally, the requirements outlined in section 2.1 further constrain the available choices: the adhesive must have a high mechanical strength, be thermally stable to survive subsequent soldering of the cantilever, and resist immersion in cleaning solvent mixes.

Given these considerations, we chose our adhesive materials amongst high-temperature curing epoxies, which exhibit the right combination of strength, stability and long pot life.

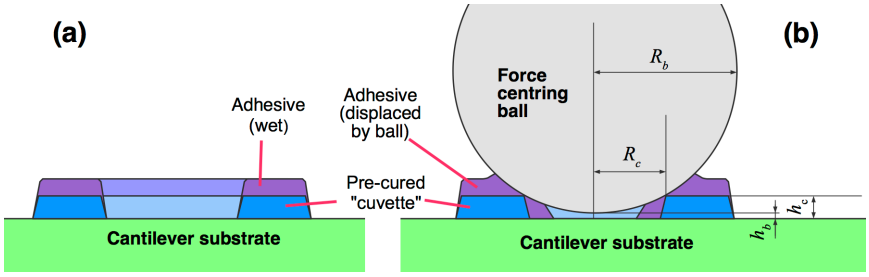

Figure 4. Positioning principle: a) deposition of "cuvette" + "adhesive" layers; b) principle of centring by cuvette & bonding by adhesive (displaced by ball).

2.3. Positioning of the balls

The chosen heat-cure epoxies do have one drawback: positioning of the ball is difficult, even with a combination of precise placement onto the cantilever and a thixotropic composition, as the adhesive will first become quite liquid upon heating, before the cure sets in (see also discussion). Therefore, we conceived a double-layer method, described in table 3 & figure 4, consisting of first depositing and curing a resin rim forming a "cuvette", then depositing the actual adhesive layer for the ball using the same mask. The pre-hardened cuvette solves two issues: 1) it acts as a mechanical centring device for the ball, and 2) it provides additional material needed for bonding over a larger area, i.e. a higher bond strength.

From figure 4, the condition for proper guiding of the ball (radius = R_b) by the cuvette (inner radius of layer = R_c; height = thickness = h_c) is for the ball to rest on the cuvette rim, i.e. the thus defined height of the bottom of the ball with respect to the cantilever surface, h_b, should not be below zero:

$$0 \le h_b = h_c + \sqrt{R_b^2 - R_c^2} - R_b \qquad (1)$$

If R_c is small vs. R_b, (1) may be approximated by the following expression, which illustrates the roughly quadratic dependence of minimal cuvette thickness h_c on its contact radius R_c:

$$0 \le h_b \cong h_c - \frac{R_c^2}{2R_b} \qquad (2)$$

3. Experimental

3.1. Paste formulation

The starting resins used were two-component Epo-Tek epoxies (Epoxy Technology, Billerica, USA): 354T, H70S, H70E and H70E2. To adjust rheology, various additives were used: α-Al_2O_3 powder (Alfa Aesar #45482, ~0.8-1 μm particle size, Karlsruhe, Germany), ethylcellulose EC-300-48 (300 mPa·s for 5% in 80:20 toluene : ethanol, 48% ethoxyl, #200654, Sigma-Aldrich, Buchs, Switzerland), amyl acetate, and 1-octadecanol (C18E0). To prepare the pastes, both components of the epoxy resin and additive(s) are first hand mixed, then run through an Exakt 50 three-roll mill (Exakt, Norderstedt, Germany).

3.2. Printing geometry

The same design was always used for the cuvette and adhesive, as this avoids a change of screen between both steps. The R_c parameter (figure 4) was varied from 150 μm to 275 μm in 25 μm increments. The basic design for the first studies is a circle (see figures 4 and 5). In a second test series, the effect of the design is examined, comparing this circle to a triangle and a square; in these latter cases, R_c corresponds to the radius of the inscribed circle.

3.3. Sample fabrication

Round, 1 mm diameter balls of five materials (steel – 100Cr6, alumina, yttria-stabilised zirconia, soda-lime glass and borosilicate glass) were bonded onto blank alumina substrates, using the procedure detailed in table 3. Screen printing (Aurel 900, Aurel Automation, Modigliana, Italy) was carried out with several stainless steel wire mesh screens (table 4) in order to optimise the compromise between thickness of deposited paste and feature definition. Throughout this work, screens are designated by two numbers, with the first being the meshing density of the stainless steel wire ('mesh'), in lines per inch, and the second the emulsion film thickness ('μm'). Please refer to reference work on screen printing [15, 16]) for more details.

Table 4. Printing screens.

Designation	Wire pitch [μm]	Emulsion thickness [μm]
325 mesh / 40 μm	78	40
200 mesh / 60 μm	127	60
135 mesh / 80 μm	188	80

3.4. Characterisation

Cuvette thickness was measured with an optical profilometer (Surface Profile Measurement Station, Breitmeier, Ettlingen, Germany). Centring of the balls was qualitatively evaluated optically with a stereo microscope. Although this method seems rather crude, ball misalignment is easy to spot in practice, as the lateral freedom of the ball increases rapidly when cuvette thickness drops below the minimum value needed to achieve correct guidance.

Mechanical strength of the adhesive bond was measured by shearing with a Royce Instruments (Napa, USA) 552 tester, with a 50 kgf (~490 N) shear head, which was also used to test the compressive strength of glass balls. Bond shear strength was also tested after thermal cycles and exposure to solvents, simulating the subsequent soldering and cleaning steps in sensor fabrication.

4. Preliminary tests – single paste formulation for both 'cuvette' & 'glue' layers

In this first test series, the effect of cuvette radius and thickness as well as paste formulation is ascertained, with the same formulation used throughout, i.e. identical 'cuvette' and 'glue' inks.

4.1. Preliminary tests of cuvette formation

A first optimisation of paste formulation and cuvette parameters was carried out for a screen-printed resin cuvette (circular shape), printed with a 325 mesh / 40 μm screen. The fine screen used here was found to be necessary for correct deposition of the smaller circles (tests with the coarse screens tended to yield full disks for small R_c values). 'Cuvette' paste formulations were formulated by loading Epo-Tek 354T with various amount (% of total mass) Al_2O_3 powder. The resulting print quality is shown in figure 5, for 7 resin layers, each cured 10 min at 150°C and for alumina loading levels of 0% (neat resin), 30% and 50%. While the neat resin is thixotropic during screen printing, it becomes quite liquid and flows excessively upon heating before setting, which prompted us to load it with alumina. A loading of 50% of total mass was found to yield the best shape retention, albeit with some flow; going

further to 60% loading caused gaps in the printed pattern to frequently occur (the corresponding image in figure 5 is for single print with a coarser screen). The printed thickness with the 325 mesh / 40 μm screen varied somewhat, at typically 20 μm for one layer, and with 15-20 μm for each additional one (~120 μm for 7 layers) – see also table 5.

The result of the evaluation of ball centring is given in table 5, for 0% and 50% alumina loading, as a function of the number of deposited cuvette layers (thickness). Accounting for process variations, the results for 50% alumina roughly agree with the prediction of (2). The approximately one more layer needed for the neat resin (0%) illustrates the effect of the resin flowing (figure 5) during heat cure in shifting the effective R_c to higher values.

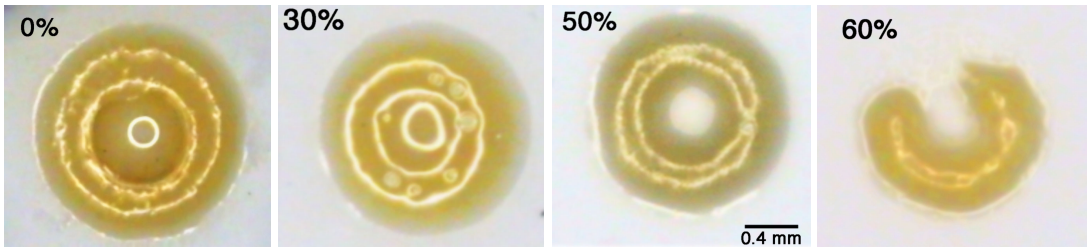

Figure 5. Cuvette formation of Epo-Tek 354T loaded with various amounts (by overall mass) of Al_2O_3 powder, after curing for 10 min at 150°C. 0-50%: 7 layers with 325 mesh / 40 μm screen; 60%: single print with 135 mesh / 80 μm.

Table 5. Centring of the balls for Epo-Tek 354T with 0% & 50% alumina loading.

Layers	Thickness		Correct centring (Y = yes; N = no), for 0% / 50% mass Al_2O_3					
(cuvette)	[μm]	R_c =	150 μm	175 μm	200 μm	225 μm	250 μm	275 μm
1	~20		Y / Y	Y / Y	Y / Y	Y / Y	N / N	N / N
2	~40		Y / Y	Y / Y	Y / Y	Y / Y	N / Y	N / N
3	~55		Y / Y	Y / Y	Y / Y	Y / Y	Y / Y	N / Y
4 & more	≥70		Y / Y	Y / Y	Y / Y	Y / Y	Y / Y	Y / Y

4.2. Effect of radius and thickness on shear strength – neat 354T & 50% alumina

The cuvettes were then overprinted with one 'glue' layer having the same composition as the cuvette, for two series: neat 354T (0%) or 50% Al_2O_3, without changing the screen (325 mesh / 40 μm). Steel balls were placed and the assemblies were cured 10 min at 150°C.

The shear strength values for 50% Al_2O_3 are all low, between less than 1 N to max. ~4 N: while this formulation is adequate to form the cuvette shape, the high filler level and low flow reduces bonding with the ball, i.e. it does not work well as a 'glue' layer.

Neat 354T is the opposite, i.e. behaves poorly as a 'cuvette' layer, but achieves good bonding with the ball. This allows seeing the effect of the cuvette parameters (figure 6) on strength. Although only conditions ensuring centring (table 5) were chosen, low cuvette thicknesses yielded low strength values. Moreover, this dependence is much more pronounced for large R_c values. Obviously, neat 354T cuvettes flow excessively, and thus strongly depart from the idealised shape shown in figure 4, yielding bonding only on the bottom surface, which is unfavourable for achieving high shear strength. This issue is compounded by the small amount of resin added by the wet 'glue' layer in this test, due to the fine screen used (325 mesh / 40 μm).

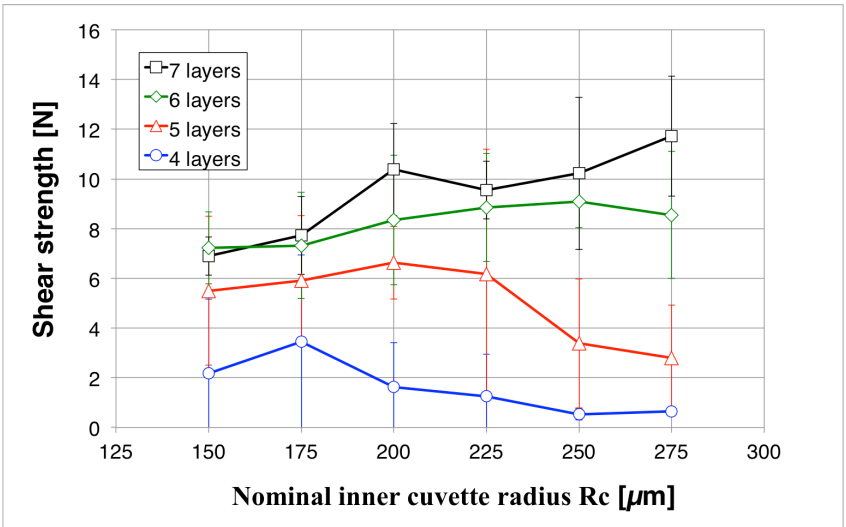

Figure 6. Shear strength of steel ball vs. nominal inner cuvette radius and number of cuvette layers (neat Epo-Tek 354T 'cuvette' and 'glue' layers, 325 mesh / 40 μm screen). Values & error bars: averages ± standard deviation; lines shown to guide the eye.

4.3. Conclusions of first tests

From this first test series, we may arrive at the following conclusions:

- It is more favourable to use different formulations for both 'cuvette' and 'glue' layers, as they require partly contradictory properties (i.e. low vs. higher flow upon cure).
- A high degree of embedding of the ball is conducive to high shear strength; this is favoured by using a high R_c value, depositing a thick cuvette, and presumably also by having a sufficiently thick final "glue" layer to accommodate any imperfections.

5. Tests with separate 'cuvette' and 'glue' compositions

Based on the results of the first series of tests, we first retain the 354T resin loaded with 50% Al_2O_3 for forming the cuvette, and separately optimise the adhesive for the 'glue' layer. After tests with the different screens (table 4), the coarsest one, 135 mesh / 80 μm was chosen, allowing to rapidly build up cuvette thickness and also giving a thick 'glue' layer. Such a screen restricts R_c to ≥ 200 μm, which is not an issue as we aim for high R_c values. Curing was as before, i.e. 10 min at 150°C, for both 'cuvette' and 'glue' layers.

5.1. Positioning issue with a large amount of glue – evacuation of excess adhesive

A first test was carried out with steel balls, 2 'cuvette' layers, and neat 354T as 'glue'. With a higher thickness of 'glue' layer from the coarser screen, another issue came up: if the ball was placed off-centre, some positioning error remained after curing, although the layers were thick enough to satisfy the centring criterion (see 4.1). This was interpreted as a result of constricted flow and the high amount of glue (figure 7): as the ball progressively settles into the cuvette, the gap with the cuvette wall becomes smaller, and further settling is impeded, eventually retaining some of the positioning error, an issue expected to be even more acute with lighter balls, e.g. glass.

As we want to retain the favourable coarse screen and large amount of adhesive (fewer process steps and high shear strength due to extensive encapsulation of the ball), we addressed this issue by promoting evacuation of the 'glue' layer as the ball settles, in two ways: 1) using a lower-viscosity 'glue' composition, and 2) using a square or triangular geometry (figure 8), conserving the positioning function but allowing easier outflow of adhesive at the corners.

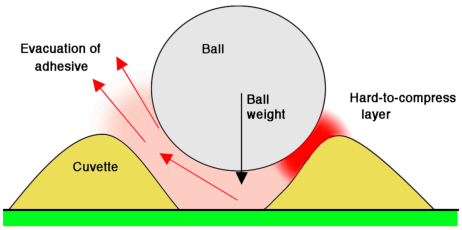

Figure 7. Illustration of impeded adhesive evacuation during settling of the ball.

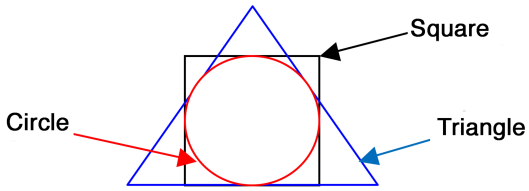

Figure 8. Triangle and square shapes, tested in addition to basic circle.

5.2. Neat H70S glue - effect of cuvette height and ball material for circular cuvettes

We first examine the approach of keeping a circular cuvette (two 354T-alumina layers, also with one for steel balls), but with a lower-viscosity H70S adhesive, and examining the effect of ball material. For steel balls, a single 'cuvette' layer was also tried.

The resulting shear strength values, shown in figure 9, all lie considerably above the specified 4 N minimum. The steel balls behave somewhat as in the first tests: increasing R_c yields higher strength for deep cuvettes (C2) and lower strength for shallower ones (C1), although the results remain acceptable here thanks to the thick deposits resulting from printing with the 135 mesh / 80 μm screen, and the better-defined cuvette shape resulting from using separate 'cuvette' and 'glue' formulations.

With two cuvette layers, the steel balls tend to yield the best strength values. It is tempting to ascribe this to their higher density, causing them to better sink into the wet 'glue' layer, achieving better embedding into the cuvette. While this may be a factor, there is no discernible effect of density on strength for the other materials (density: steel > zirconia > alumina > both glasses), and surface tension effects presumably also play a role. Interestingly, rupture tends to occur not at the ball – glue interface, but between the 'glue' and 'cuvette' layers, possibly meaning that the alumina loading of the latter may be somewhat too high. As expected, the low glue viscosity yielded good ball centring.

In spite of the apparently good results shown here, the tested configuration is not practicable, as H70S is insufficiently viscous at room temperature, and seeps through the coarse screen, requiring frequent cleaning: a somewhat more viscous resin is necessary, which may however reintroduce the issue of glue evacuation described in 5.1.

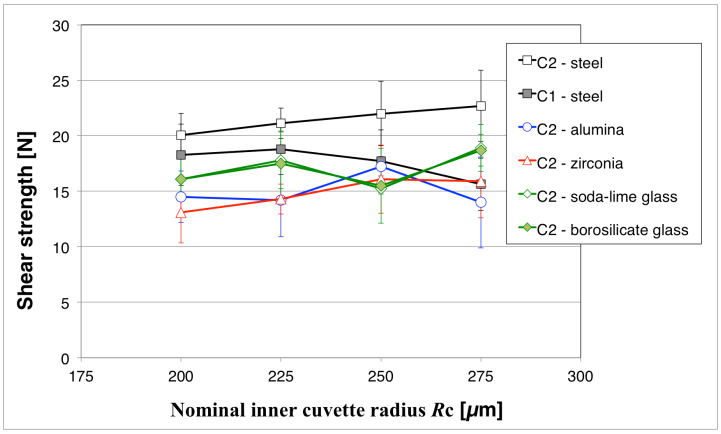

Figure 9. Shear strength for circular geometry (larger designs) vs. ball material, inner cuvette radius R_c and (for steel) number of cuvette layers (C1 = 1, C2 = 2), for Epo-Tek 354T & 50% Al_2O_3 cuvette and H70S glue, both printed with 135 mesh / 80 μm screen. Values & error bars: averages ± standard deviation; lines shown to guide the eye.

Figure 10. Shorn-off balls, showing rupture mostly between 'cuvette' and 'glue' layer.

5.3. Optimisation of 'glue' layer with 135 mesh / 80 µm screen and square geometry

To ensure good evacuation of adhesive (as we seek a somewhat more viscous one than H70S), we decided to carry out the next tests with triangular and square cuvettes (and glue) printed layers (figure 8), choosing R_c = 250 µm, one of the larger values. While first tests [14] showed favourable centring and embedding behaviour for both triangles and squares, the square form was preferred in terms of visual centring and screen printing (as the screen mesh consists of two sets of wires at a 90° angle to each other, all lines are equivalent for a square, but not for a triangle).

We compared here six 'glue' compositions, with 2 'cuvette' layers of 354T & 50% Al_2O_3, as before, and using soda-lime glass (both smooth and matte finish) and steel balls: the original H70S (1), H70E (2), H70E2 (3), and H70S mixed with 1% (4), 3% (5) and 6% (6) C18E0. C18E0 was mixed in the molten state (~60-70°C) into the resin component of H70S, and the beaker was cooled with water while mixing; this results in a fine suspension of C18E0, enhancing the viscosity at room temperature (i.e. C18E0 acts as a filler) but enhancing flow during heating, as C18E0 then melts and rather acts as a solvent, in the same vein as our previous work with C18E0 and other such waxy materials [17, 18].

Shear strength was measured both in the cured state (10 min at 150°C), and after further heat treatment, 5 and 15 min at 260°C, which considerably exceeds the actual time of further soldering operations (<1 min at ~260°C). Tests were also made to simulate cleaning operations: 30 min ultrasound bath, immersed in solvents (universal thinner, solder flux cleaner and isopropanol).

The results (figure 11) show high strength for all tested compositions, except H70S loaded at 3% and 6% with C18E0 together with the glass balls, which rupture by separation with the ball: C18E0 presumably migrates out of the resin and forms a low-strength layer there. This issue was not seen with 1%, which nevertheless sufficiently increased the viscosity of H70S to make it printable. Heat treatment was not deleterious; on the contrary, strength levels rather tended to increase by further curing of the resins. Immersion in solvents [14] (results not shown here) had no visible effect.

Based on these results, we chose the commercial adhesive with the best printability, H70E2.

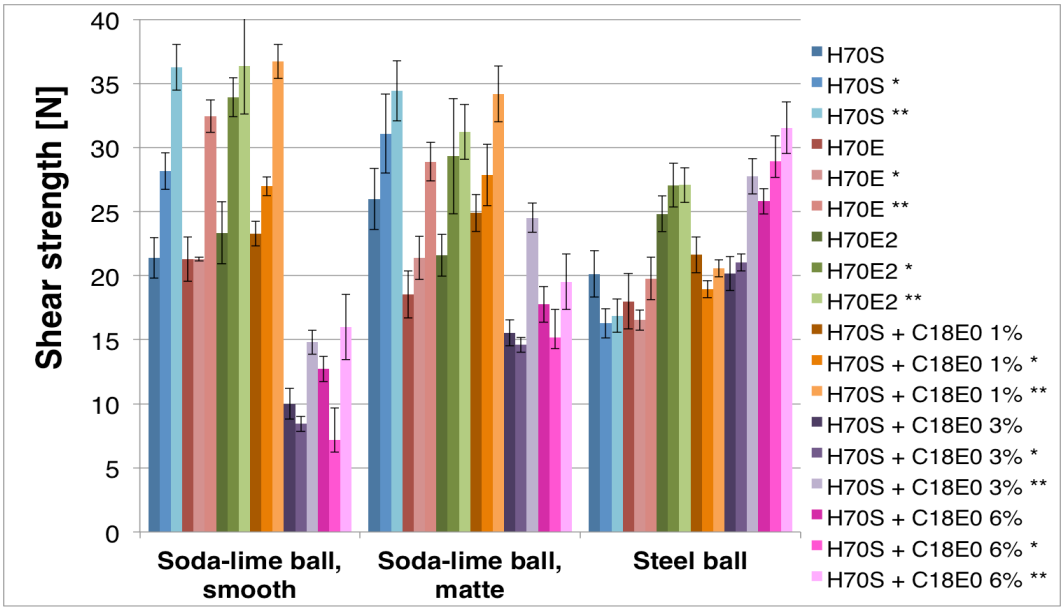

Figure 11. Shear strength (average ± standard deviation) for square geometry (R_c = 250 µm) vs. ball material, 'glue' formulation and heat treatment: initially cured 10 min at 150°C, then treated 5 min (*) or 15 min (**) at 260°C. Cuvette = 2× 354T & 50% Al_2O_3; printing with 135 mesh / 80 µm screen.

5.4. Further optimisation of 'cuvette' layer with 135 mesh / 80 µm screen and square geometry

As the previously-retained 'cuvette' composition (354T & 50% Al_2O_3) tended to form somewhat irregular shapes with the coarse 135 mesh / 80 µm screen, a finer evaluation of filler level was made: 40%, 45%, 50% and 55% Al_2O_3. As seen in figure 12, such formulations result in bleeding (low filler level), or in insufficient smoothing out of the screen irregularities (high level), with 50% turning out to be the best compromise, as before; therefore, a more advanced formulation was developed, with 41% Al_2O_3 in conjunction with 1.7% EC-300-48 and 3% amyl acetate added into the resin component of 354T (incorporated as a solution in acetone, which evaporates during mixing). EC-300-48 considerably increases the room-temperature viscosity, which is partly counteracted by the amyl acetate solvent. Upon heating, amyl acetate evaporates, leaving EC-300-48 only and thus restricting bleeding; this clearly results in the best print quality, as shown in the last image of figure 12. This optimised 'cuvette' formulation did not significantly impact the bond shear strength, as the results of a confirmation test show in figure 13.

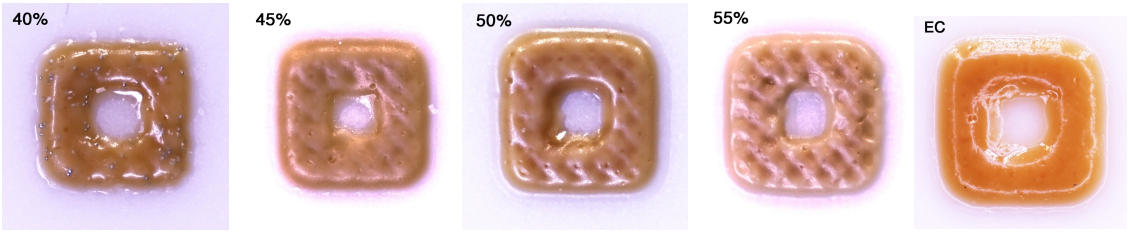

Figure 12. Cuvette formation (one layer printed with 135 mesh / 80 µm screen) of Epo-Tek 354T, loaded with various amounts (percentage of overall mass) of Al_2O_3 powder, after curing for 10 min at 150°C; "EC" = with 41% Al_2O_3 and 1.7% EC-300-48.

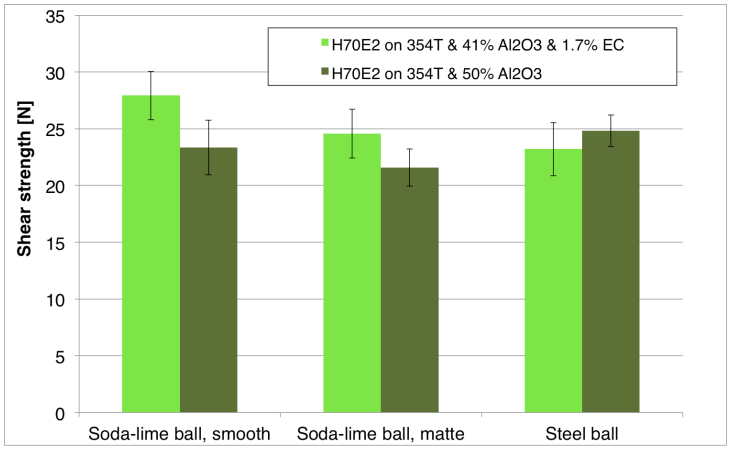

Figure 13. Shear strength (same conditions as figure 11) for as-cured H70E2 'glue' layer, comparing original 'cuvette' formulation (354T with 50% Al_2O_3 filler) with optimised one (354T with 41% Al_2O_3 and 1.7% EC-300-48, with additional 3% amyl acetate that evaporates during curing).

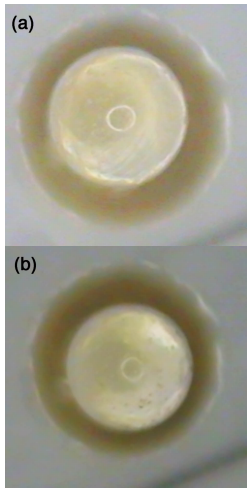

Figure 14. Glass balls after compression test at 30 N (a) and 50 N (b), with no visible damage (white circles in centre due to reflections).

6. Compression of glass balls

Finally, a compression test was carried out on the soda-lime glass balls against a relatively hard tool steel surface. The glass balls were adhesively bonded onto an alumina substrate, which was held by the tester vice with several backing substrates to enhance its strength.

In a single cycle, no visible damage to the ball was observed up to ~50 N, i.e. 25× the maximal force range of the sensor (2 N), as attested by figure 14. At this point, the pile of substrates backing the ball broke, ending the test. Performing 5 cycles with 15 N [14] also did not visibly damage the ball. Therefore, the low-cost glass balls are deemed acceptable for our application.

7. Conclusions and outlook

A simple and straightforward adhesive bonding process has been developed to replace solder attachment, and shown to yield acceptable shear strength levels. Compared to soldering of the ball, adhesive bonding entails significantly simpler processing. Additionally, the bottom cantilever mounting pads experience two vs. three reflow steps, i.e. only those necessary for 1) pre-tinning and 2) solder attachment, reducing solder oxidation and metallisation leaching issues, translating into lower fabrications costs and higher process reliability.

The process consists in two printing steps of two different epoxy-based compounds, in order to duplicate the twin functionality of the solder: centring of the ball (by a first 'cuvette' formulation) and actual attachment (with a 'glue' one). The resulting penalty is relatively small, however, as they are performed with the same screen, requiring only summary cleaning and flushing of the screen when switching from one process to the other. Other alternatives (e.g. precise pick-and-place of the ball with a UV glue) could also be used.

Acknowledgments

The authors are indebted to M. Garcin for help in carrying out the experiments.

References

[1] Morten B and Prudenziati M 1994 Piezoresistive thick-film sensors *Handbook of Sensors and Actuators vol. 1: Thick film sensors* ed M Prudenziati (Amsterdam: Elsevier) pp 189-208

[2] White NM and Turner 1997 Thick-film sensors: past, present and future *Measurement Science and Technology* **8** 1-20

[3] White NM 2007 Advances in thick-film sensors *Proc. 14th Int. Conf. on Solid-State Sensors, Actuators and Microsystems - Transducers / Eurosensors'07* (Lyon, France) (Piscataway: IEEE) pp 107-11

[4] Partsch U, Lenz C, Ziesche S, Lohrberg C, Neubert H and Maeder-T 2012 LTCC-based sensors for mechanical quantities *Informacije MIDEM - Journal of Microelectronics, Electronic Components and Materials* **42** 260-71

[5] Maeder T 2011 Ceramic modules for sensors, fluidics & packages in harsh environments *MEMS Technology Review* **8** 10-3

[6] Maeder T, Fahrny V, Stauss S, Corradini G and Ryser P 2005 Design and characterisation of low-cost thick-film piezoresistive force sensors for the 100 mN to 100 N range *Proc. XXIX Int. Conf. of IMAPS Poland* (Koszalin) pp 429-34

[7] Maeder T, Jacq C and Ryser P 2014 Thick-film load-sensing bridges – effect of temperature and mechanical boundary conditions *Procedia Engineering* **87** 180-3

[8] Jurków D, Maeder T, Dąbrowski A, Santo Zarnik M, Belavič D, Bartsch H and Müller J 2015 Overview on low temperature co-fired ceramic sensors *Sensors and Actuators A* **233** 125-46

[9] Birol H, Maeder T, Nadzeyka I, Boers M and Ryser P 2007 Fabrication of a millinewton force sensor using low temperature co-fired ceramic (LTCC) technology *Sensors and Actuators A*

134 334-8
[10] Jacq C, Maeder T and Ryser P 2011 Signal stability of LTCC cantilever force sensors *Procedia Engineering* **25** 551-4
[11] Jacq C, Maeder T, Haemmerle E, Craquelin N and Ryser P 2011 Ultra-low pressure sensor for neonatal resuscitator *Sensors and Actuators A* **172** 135-9
[12] Nousiainen O, Kangasvieri T, Rönkä K, Rautioaho R and Vähäkangas J 2007 Interfacial reactions between Sn-based solders and AgPt thick film metallizations on LTCC *Soldering & Surface Mount Technology* **19** 15-25
[13] Achmatowicz S and Zwierkowska E 2006 Lead free thick film circuits *Materiały Elektroniczne* **34** 5-47
[14] Blot M 2014 Collage de billes sur le capteur de force MilliNewton [Adhesive bonding of balls on the MilliNewton force sensor] *Student project in microtechnology, EPFL, Laboratoire de Production Microtechnique, Lausanne, Switzerland*
[15] Sergent JE 2007 Screen printing, *Ceramic interconnect technology handbook*, ed FD Barlow A Elshabini (Boca Raton, USA: CRC Press), Chapter 5, pp 199-233
[16] Miller LF 1969 Paste transfer in the screening process, *Solid State Technology* **12** 46-52
[17] Maeder T, Jacq C, Ammon L and Ryser P 2014 Tuneable PTC effect in polymer-wax-carbon composite resistors", Microelectronics International 31 (3), 143-148, 2014.
[18] Maeder T, Jiang B, Vecchio F, Jacq C, Ryser P and Muralt P 2012 Lamination of LTCC at low pressure and moderate temperature using screen-printed adhesives *Proc., 8th Int. Conf. on Ceramic Interconnect and Ceramic Microsystems Technologies (CICMT)* (Erfurt, Germany) pp 348-352